Electronic Supplementary Information (ESI)

Crystallization of citrate-stabilized amorphous calcium phosphate to nanocrystalline apatite: a surface-mediated transformation

Konstantinos Chatzipanagis[a,§], Michele Iafisco[b,§], Teresa Roncal-Herrero[a], Matthew Bilton[a,c], Anna Tampieri[b], Roland Kröger[a,*] and José Manuel Delgado-López[d,*]

[a]Department of Physics, University of York, York, United Kingdom.

[b]Institute of Science and Technology for Ceramics (ISTEC), National Research Council (CNR), Faenza, Italy

[c]Department of Chemistry, Simon Fraser University, Burnaby, Canada.

[d]Laboratorio de Estudios Cristalográficos, Instituto Andaluz de Ciencias de la Tierra (IACT, CSIC-UGR), Armilla, Granada, Spain.

*Corresponding authors: R. Kröger (roland.kroger@york.ac.uk) and J.M. Delgado-López (jmdl@iact.ugr.csic.es)

Materials and Methods

Synthesis of citrate functionalized amorphous calcium phosphate (cit-ACP) nanoparticles

Cit-ACP particles were synthesized by the bath precipitation method described elsewhere (Delgado-López et al. 2012, Delgado-López et al. 2014). Briefly, two solutions of (i) 0.1 M $CaCl_2$ + 0.4 M $Na_3C_6H_5O_7$ and (ii) 0.12 M Na_2HPO_4, + 100 mM Na_2CO_3 were mixed (1:1 v/v, 200 mL total) at room temperature. The pH was adjusted with HCl to 8.5. The precipitation of cit-ACP occurred immediately after mixing. The precipitates were immediately removed from the mother solution by centrifugation (9000 rpm, 3 minutes) and then repeatedly washed with ultrapure water by centrifugation. Subsequently, they were freeze-dried overnight and stored at 4 °C for further characterizations. All the solutions were prepared with ultrapure water (0.22 μS, 25 °C, MilliQ, Millipore). Calcium chloride dehydrate ($CaCl_2.2H_2O$, Bioxtra, ≥99.0% pure), sodium citrate tribasic dehydrate, $Na_3C_6H_5O_7\cdot2H_2O$, ACS reagent, ≥99.0% pure), sodium phosphate dibasic (Na_2HPO_4, ACS reagent, ≥99.0% pure) and sodium carbonate monohydrate ($Na_2CO_3\cdot H_2O$, ACS reagent, 99.5% pure) were supplied by Sigma-Aldrich.

Ex-situ TEM observations

Transmission electron microscopy (TEM) was used to study *ex situ* the morphological evolution from cit-ACP to Ap. Cit-ACP suspensions (0.5 mg mL^{-1}) were prepared in ultrapure water or

Phosphate Buffer Solution (PBS 1x, 137 mM NaCl, 2.7 mM KCl, 10 mM Na_2HPO_4 and 1.8 mM KH_2PO_4, pH = 7.3 ± 0.01). After the desirable elapsed time, the suspensions were drop-casted onto lacey carbon copper grids. The excess of water and/or PBS was absorbed by powder-free paper tissue allocated under the grid. This process led to a rapid removal of the solution. The samples were then air-dried and images were collected using a conventional TEM JEM 2011FS with LaB_6 source operated at 200kV. Selected Area Electron Diffraction (SAED) patterns of selected samples were also acquired.

Time-dependent in-situ Raman Spectroscopy

In situ time-dependent Raman spectroscopy was used to monitor the transition from cit-ACP to Ap in both media. All experiments were performed by preparing suspensions of 0.5 mg cit-ACP mL^{-1}. ACP suspensions were drop-cast between a glass slide and glass slip which were carefully sealed with vacuum grease in order to prevent evaporation during the acquisition. Immediately after, Raman spectra were sequentially collected under back scattering geometry using a LabRAM-HR (Jobin–Yvon, Horiba) dispersive Raman spectrometer. A diode-pumped 532 nm wavelength laser with an output of 20-25 mW was used as the excitation source and was focused through a 50x objective (Olympus) providing a sample spot of ~ 1µm. The Raman signal was detected by a Peltier CCD detector (1064 × 256 pixels) and averaged over 2 scans for 250 seconds. A spectral range from 200 to 3700 cm^{-1} and a diffraction grating of 600T grooves/mm were used.

pH Evolution

The pH evolution during the ACP to crystalline transformation was continuously monitored at 25 ºC using a Titan X pH meter (Sentron) equipped with a Sentron micro-electrode. The electrode was previously calibrated using standard buffer solutions (pH 4.00, 7.00, and 10.00 at 25 ºC, Sentron) with an average error of 0.01 pH units.

Zeta potential of cit-ACP

Zeta potential of cit-ACP in water was measured at 25 °C as electrophoretic mobility with a Zetasizer Nano analyzer (Malvern, UK) using disposable folded capillary cells. Zeta potential average and zeta potential deviation values are given.

Assignment of Raman bands

The phosphate bands are the following (Tarnowski et al 2002, Yilmaz and Evis 2014, Yamini et al. 2014, Ciobanu et al. 2013): v_1 stretching mode (945-960 cm^{-1}), v_2 double degenerate bending mode (420-455 cm^{-1}), v_3 triply degenerate anti-symmetric stretching mode (1020-1077 cm^{-1}) and v_4 triply degenerate bending mode (570-620 cm^{-1}). In addition to the phosphate bands, other vibrational modes related to the presence of citrate in the particles were observed[1]: COO bending mode (843-847 cm^{-1}) and CH$_2$ stretching mode (2928-2933 cm^{-1}). The water band originated from the surrounding liquid environment during the experiment was attributed to the O-H stretching mode (3225-3233 cm^{-1} and 3425-3435 cm^{-1})(Yeung and Chan 2010). The main Raman bands are summarizes in Table S1 below.

Table S1. Raman bands frequency – Assignment of bands

Bands Position (cm^{-1})	Assignment
420 - 450	v_2 PO$_4$ bending mode
570 - 620	v_4 PO$_4$ bending mode
843 - 847	δ COO bending mode of citrate
945 – 953 957 - 960	v_1 PO$_4$ stretching mode
1020 - 1077	v_3 PO$_4$ anti-symmetric stretching mode
2928 - 2932	v CH$_2$ stretching mode of citrate
3225 – 3233 3425 - 3435	v O-H stretching mode

Determination of position and FWHM of Raman peaks

Spectral decomposition and data fitting were performed to separate the individual bands and determine the characteristics of the v_1 PO$_4$ Raman envelope. In the case of cit-ACP in water, a single symmetric band was observed during the early stages of crystallization (0-775 min) as a result of the presence of solely an amorphous phase. The values for the location, intensity and width of this single amorphous band for each measurement were estimated by non-linear curve fitting. The mean values for both position and width were then calculated and the extremes were considered as the highest and lowest fitting values observed. Thus, these mean

values (as well as the extremes) for the location and width of this band formed the range of constraints (error bars) when fitting the additional crystalline band during decomposition. To perform the fitting process more efficiently, the decomposition and curve fitting was initially done on the last measurements where the crystalline band was more prominent and well-defined. This crystalline Raman band was freely iterated until the optimum fitting outcome was achieved. The mean and the extreme (highest and lowest) values for the location and width of the crystalline band were estimated as a result of the corresponding mean and extreme values of the ACP Raman band. The next step was to fit all the remaining intermediate spectra by keeping these values (for location and width) of both bands constant and thus determine the variation in the relative intensities and resulting areas between these bands.

Since we are investigating a series of related measurements where the initial cit-ACP is accompanied by the development of a well- defined crystalline phase with increasing maturation time, the location and width of the corresponding Raman bands can be kept fixed and thus monitor the transition from one phase to the other by investigating the relative variation of areas of these bands (Meier, 2005). For decomposition and non-linear curve fitting, Igor Pro 6.34 software was used. The Raman fitting of solid cit-ACP and Ap in both solutions was performed using Gaussian profiles (Bradley & Krech, 1992). An example of fitting with Igor Pro 6.34 is given below. The blue fit corresponds to the Gaussian model and the green line represents the linear baseline that was simultaneously applied during the fitting process. The residuals after the fitting can be also seen.
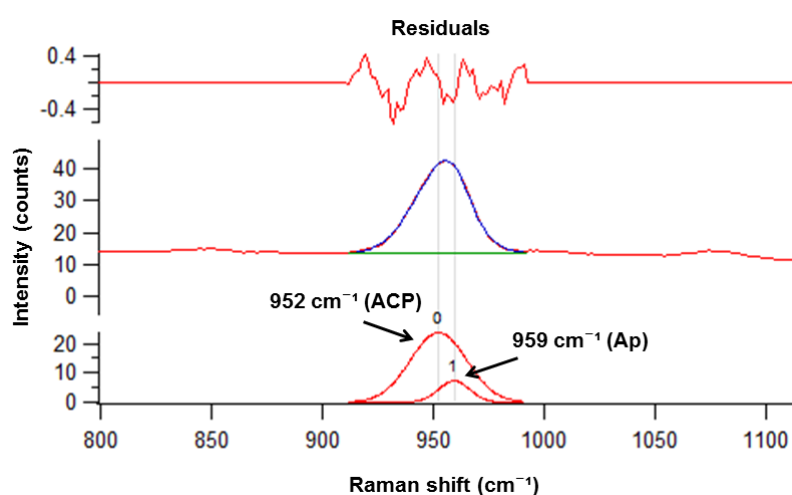
Figure S1. Non-lineal c*urve fitting (decomposition) of the $\nu_1 PO4$ stretching Raman peak. The fittings were performed with the Igor pro 6.34 software.*
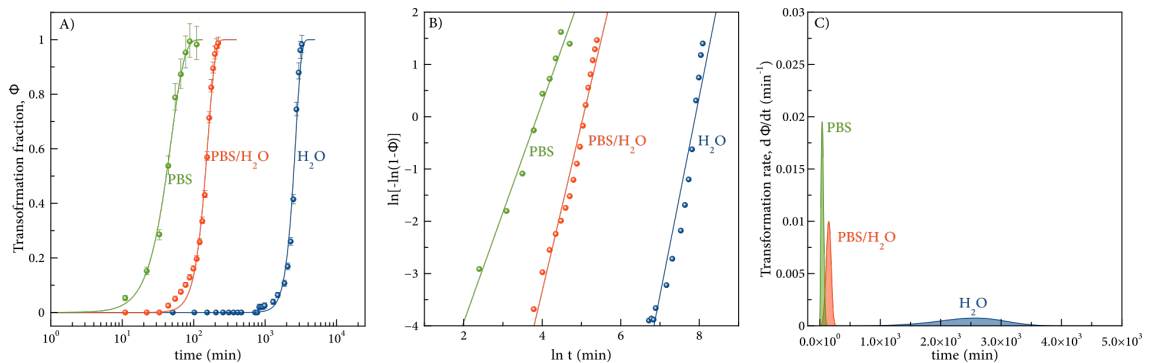
Figure S2. *(A) Avrami fits to the data obtained in the case of pure PBS, a PBS/water mixture (1:1) and pure water. (B) Plots of the linearized Avrami equation (ln[-ln(1-Φ(t))] vs ln(t)). C) Time derivative of the Avrami-fit of Φ(t).*
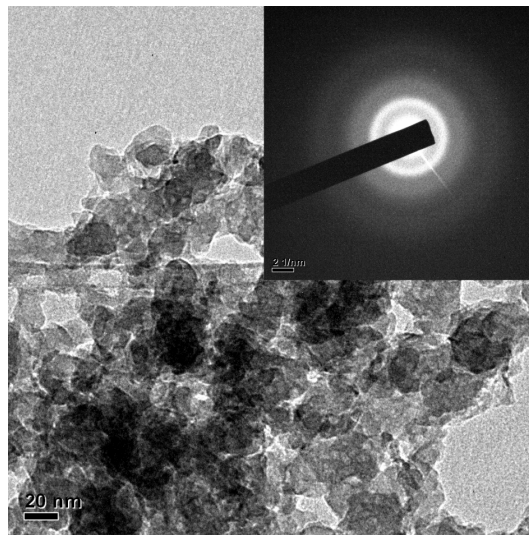
Figure S3. *TEM micrograph and the corresponding SAED pattern of the amorphous particles obtained after 2 days of the immersion of cit-ACP in water.*
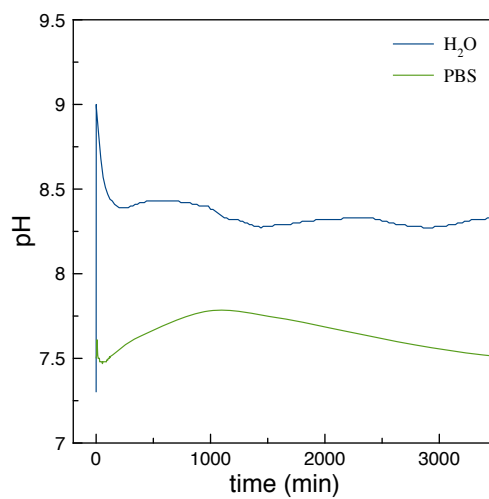
Figure S4. *pH evolution during ACP transformation in water and PBS.*

Movie S1. Time-lapse optical microscopy imaging during cit-ACP transformation in water.

Cit-ACP transformation in water was recorded by time-lapse optical microscopy using a Nikon AZ100 microscope since the immersion of cit-ACP in water (t=0) until the full transformation (5 days). The initial shape of the cit-ACP particles remains after 5 days, which excludes the total dissolution and further recrystallization of cit-Ap. Conversely, the particles become clearer during the conversion. This could be possibly due to changes in the density of the particles because of the crystallization process.

References

1. J. M. Delgado-López, M. Iafisco, I. Rodríguez, A. Tampieri, M. Prat and J. Gómez-Morales, Acta Biomater., 2012, 8, 3491-3499.
2. J. M. Delgado-López, R. Frison, A. Cervellino, J. Gómez-Morales, A. Guagliardi and N. Masciocchi, Adv. Funct. Mater., 2014, 24, 1090-1099.
3. C. P. Tarnowski, M. A. Ignelzi and M. D. Morris, J. Bone Miner. Res., 2002, 17, 1118-1126.
4. B. Yilmaz, Z. Evis, Spectroscpy Letters., 2014, 47, 24-29.
5. D. Yamini, G. Devanand Venkatasubbu, J. Kumar, V. Ramakrishnan, Spectrochimica Acta Part A: Molecular and Biomolecular Spectroscopy., 2014, 117, 299-303.
6. C. S. Ciobanu, S. L. Iconaru, P. Le Coustoumer, D. Predoi, Journal of Spectroscopy., 2012, 2013, 1-5.
7. M. C. Yeung, C. K. Chan, Aerosol Science and Technology., 2010, 44, 269-280.
8. R. Meier, Vibrational spectroscopy., 2005, 39, 266-269.
9. M. S. Bradley, J. H. Krech, J. Phys. Chem., 1992, 96, 75-79.